

Article

Assessing the Driving Forces in Vegetation Dynamics Using Net Primary Productivity as the Indicator: A Case Study in Jinghe River Basin in the Loess Plateau

Hao Wang ^{1,*} , Guohua Liu ², Zongshan Li ², Pengtao Wang ¹ and Zhuangzhuang Wang ¹

¹ Department of Geography, School of Geography and Tourism, Shaanxi Normal University, Xi'an 710119, China; yewufeige@126.com (P.W.); Geowangzz@126.com (Z.W.)

² State Key Laboratory of Urban and Regional Ecology, Research Center for Eco-Environmental Science, Chinese Academy of Sciences, Beijing 100085, China; ghliu@rcees.ac.cn (G.L.); zsli_st@rcees.ac.cn (Z.L.);

* Correspondence: foreva@snnu.edu.cn; Tel.: +86-029-8531-0525

Received: 5 May 2018; Accepted: 19 June 2018; Published: 21 June 2018



Abstract: An objective and effective method to distinguish the influence of climate change and human activities on vegetation dynamics has great significance in the design and implementation of ecosystem restoration projects. Based on the Moderate Resolution Imaging Spectroradiometer (MODIS) remote data and the Miami and Carnegie–Ames–Stanford Approach (CASA) model, this study simulated and used net primary productivity (NPP) as an indicator to identify vegetation dynamics and their driving forces in the Jinghe River basin from 2000 to 2014. The results showed that: (1) The vegetation in the Jinghe River basin, which accounted for 84.4% of the study area, showed an increasing trend in NPP; (2) Human activities contributed most to vegetation restoration, which accounted for 54.5% of the areas; 24.0% of the areas showed an increasing trend in the NPP that was dominated by climate factors. Degradation dominated by human activities accounted for 4.3% of the study area, and degradation dominated by climate factors resulted in 17.2%; (3) The rate of vegetation degradation in areas dominated by climate factors rose with increased slope, where the arid climate caused shortages of water resources, and the human-dominated vegetation restoration activities exacerbated the vegetation's water demand further, which surpassed the carrying capacity of regional water resources and led ultimately to vegetation degradation. We recommend that future ecological restoration programs pay more attention to maintaining the balance between ecosystem restoration and water resource demand to maximize the benefits of human activities and ensure the vegetation restoration is ecologically sustainable.

Keywords: net primary productivity; Loess Plateau; climate fluctuation; human activity; vegetation restoration; simulation modeling; CASA; MODIS; remote sensing

1. Introduction

Climate and human activities are the primary driving forces of changes in terrestrial ecosystems [1–3]. Commonly, regional vegetation dynamics are related closely to changes in local climate conditions and human activities [4–6]. However, it is difficult to distinguish the influence of these two driving factors when both function in the process of vegetation growth [7]. Particularly in arid and semi-arid regions such as the Loess Plateau, the water-limited environment makes the vegetation there highly sensitive to changes in temperature and precipitation [8,9], and high-intensity human activities easily may lead to degradation of the local vegetation [10–13]. To improve the ecological environment, the local government has implemented a series of ecological restoration programs, such as the Grain for Green

Program (GGP), which complicates the effects of human activities on vegetation [14]. Our previous studies showed that the changes between different land use types contribute significantly to the changes in vegetation coverage, especially for the transformation between farmland and forests/grasslands, which were related closely to topographical factors; for example, the implementation of GGP requires that farmland with slopes between 15 to 25° are returned to grassland or forest, while farmland with slopes >25° should be returned to forest [15,16]. These ecological restoration programs have increased the coverage and net primary productivity (NPP) of vegetation in the Loess Plateau and improved the local ecological environment gradually [17,18]. However, recent studies have shown that restoration is reaching the plateau's sustainable water resource limits [19]. The water resources of the natural environment are unable to meet the growing demand of a large amount of vegetation planted recently [20]. Inappropriate selection of ecological restoration species increases the consumption of soil moisture and causes a low survival rate of revegetated trees and shrubs [21,22]. Therefore, studies that identify and quantify the effects of climate conditions and human activities on vegetation dynamics have great significance in the design and implementation of ecosystem restoration projects. The results of studies such as this will help in the selection of suitable sites and methods for ecological restoration that are adapted to local climate conditions or mitigate the negative effects of human activities, and achieve sustainable development of regional ecological restoration [23,24].

Previous studies designed to differentiate the effects of climate and human activities on vegetation dynamics have focused primarily on statistical analyses, such as principal component, correlation, and significance analyses. Limited by the study methods, these studies failed to tell us the spatial distribution pattern and the change trend of vegetation, which is driven by climate change or human activities [25–28]. With the development of remote sensing technology, recent studies have begun to use the Normalized Difference Vegetation Index (NDVI) remote data and residual analysis methods to distinguish the influence of climate conditions and human activities on vegetation dynamics [15,29]. The concept on which this method is based is that the NDVI and precipitation are correlated significantly, and based on the NDVI and precipitation data, a regression relation is established to simulate the NDVI expected. The difference between the expected and actual NDVI indicates the effect of human factors on vegetation dynamics [30,31]. However, research that relies solely on the relation between NDVI and precipitation fails to reflect temperature's influence on vegetation dynamics. Meanwhile, there are uncertainties about the results of the NDVI expected, which is calculated according to the precipitation–NDVI relation, and thus, the influence of climate and human activities on vegetation dynamics cannot be differentiated fully [28,32]. Therefore, it is necessary to use an objective and effective method to distinguish the influence of the two factors on vegetation [33].

NPP is the net energy that vegetation converts through photosynthesis to biomass [34]. As an important part of ecosystem function and carbon circulation, NPP often is used as an indicator of vegetation's sensitivity to climate change and human activities [33,35]. Previous studies have adopted NPP to discriminate the response of vegetation to climate change [36,37], and today, researchers have begun to use NPP to identify the effects of human activities on vegetation dynamics [4,38]. Based on models of different ecological processes and remote sensing data, the NPP expected (NPP_e) can be calculated to simulate the climate-induced production, and the actual NPP (NPP_a) to simulate the combined induced production [39,40]. The difference between the NPP_e and NPP_a indicates the effects of human factors on vegetation dynamics. Because different ecological models are used to simulate both the NPP_e and NPP_a , the results can avoid the errors and uncertainties associated with the precipitation–NDVI linear regression method effectively [41–43]. Therefore, this study adopted NPP as an indicator to assess the driving forces in vegetation dynamics.

The Jinghe River is a secondary tributary of the Yellow River that plays an important role in the ecological security of the Loess Plateau, and both the natural environment and human activities have experienced significant changes there in recent years [44,45]. However, few studies have focused on spatial quantificational analysis of the driving forces in vegetation dynamics in this

region [46]. This study uses NPP as an indicator to identify the vegetation change trend and its driving forces in Jinghe River basin from 2000 to 2014. The ultimate objectives of this study were to: (1) explore the vegetation change trend in Jinghe River basin; (2) distinguish the role of climate change and human activities in vegetation dynamics; and (3) quantify the effects of these two factors and introduce topographical factors to determine their spatial distribution. This study can be considered a reproducible method for the analysis of driving factors in vegetation dynamics at the basin scale and provides a scientific basis for the development of local ecological restoration.

2. Data and Methods

2.1. Study Area

The Jinghe River basin is located in the southwest of the Loess Plateau and covers an area of 70,040 km² (Figure 1). The basin is in the transitional zone between the temperate semi-humid and temperate semi-arid and has a typical temperate continental climate. The temperature and precipitation in the Jinghe River basin decrease gradually from southeast to northwest. The annual average temperature and average annual precipitation in the region are approximately 10 °C and 290–560 mm, respectively. The primary vegetation types in this area are forest, shrub, and grassland (Table 1) [47]. In the past decade, high-intensity human activities in the basin have led to an increasing trend in soil erosion and decreasing trend in vegetation coverage [45]. Thus, to improve the ecological environment, the local government has implemented a series of ecological programs, such as the Grain for Green Program (GGP). However, the continuous population growth and rapidly expanding towns continue to exert considerable pressure on the natural environment [46]. Therefore, this study focused on the Jinghe River basin as the study area to analyze changes in vegetation dynamics and distinguish the effects of climate change and human activities. The results of this research are of great scientific significance in understanding the rules of regional vegetation changes, as well as summarizing and improving ecological restoration measures.

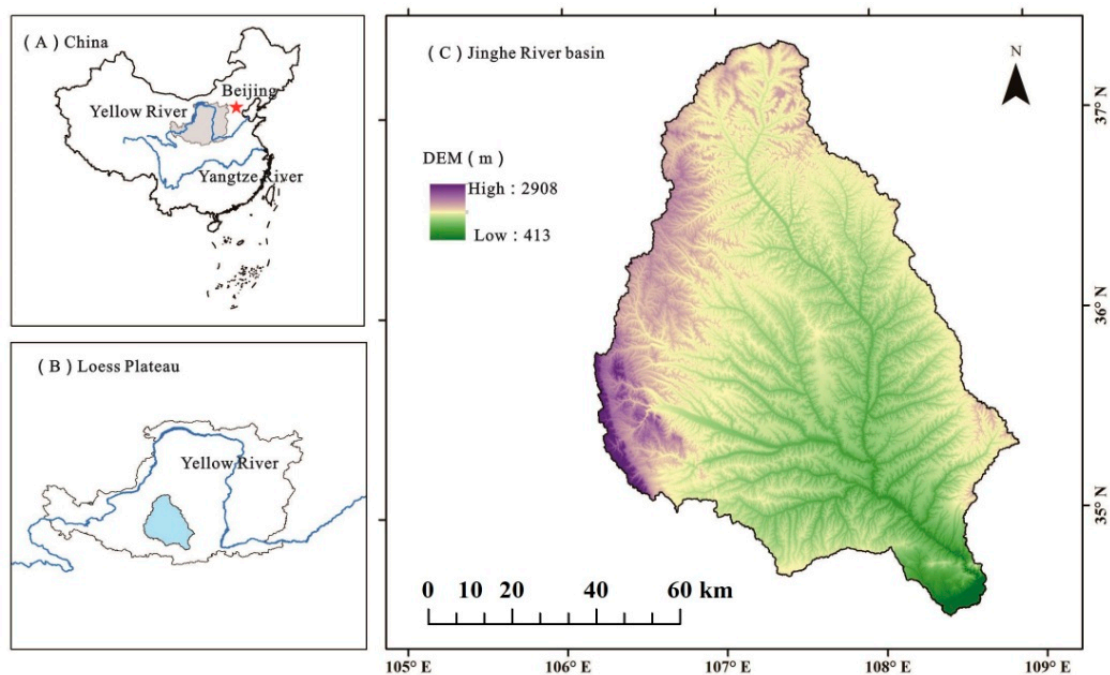


Figure 1. Location of the Jinghe River basin. DEM, Digital Elevation Model.

Table 1. The land use types in percentage terms in the Jinghe River basin (Unit: %).

Land Use Types	Forest	Shrub	Grassland	Farmland	Others
Area in percentage	28.7	10.2	32.1	27.3	1.7

2.2. Remote Sensing Data Sets

Land use map and vegetation classification map for the Jinghe River basin were obtained from the Center for Earth Observation and Digital Earth, China (<http://www.ceode.cas.cn/sjyhfw/>) (Table 1). Based on the Landsat remote data and the vegetation classification map, a series of 30 m resolution land use maps were created with an accuracy rate higher than 94%.

Temperature and precipitation were adopted in this study as the meteorological factors that affect vegetation dynamics, and the data were obtained from the China Meteorological Data Sharing Network (<http://data.cma.cn/>). The monthly temperature and precipitation data of 676 stations in China were used to calculate the spatial distribution of the meteorological factors by using ArcGIS v10.2 software (Environmental Systems Research Institute, Inc., Redlands, CA, USA) with Kriging interpolation method. The spatial resolution of the results was set to 250 m. Based on the range of the Jinghe River basin, the meteorological data for the Jinghe River basin from 2000 to 2014 were obtained using the Extract by mask function of ArcGIS. Then, the spatial meteorological data were used in the Miami model to simulate the NPP_e .

The NDVI data (2000–2014) that were used to simulate the NPP_a using the Carnegie–Ames–Stanford Approach (CASA) model were obtained from the MODIS NDVI product (MOD13Q1). This dataset can be downloaded from <https://ladsweb.modaps.eosdis.nasa.gov> and has a spatial resolution of 250 m and a temporal resolution of 16-day intervals. To reduce the noise attributable to bare soil and clouds, we converted all NDVI remote data to monthly data using the maximum value method, and eliminated those grid cells with a NDVI value less than 0.05 [48,49].

2.3. Net Primary Production Estimates

2.3.1. Estimation of the Expected NPP

The Miami model was used to estimate the NPP_e , which is affected only by meteorological factors [40]. This model is the first NPP estimation model used widely worldwide. The Miami model, which is based on Liebig's "Law of minimum" and the relation between vegetation NPP and annual average temperature and annual precipitation, was used to determine the values of NPP [50,51]. Because of its simple parameters and reasonable estimates of NPP, the Miami model has been used widely in NPP estimation studies in different regions of the world [52]. The formula of the model is as follows:

$$NPP_e = \min \left\{ \left(\frac{3000}{1 + \exp(1.315 - 0.119 t)} \right), (3000[1 - \exp(-0.000664 r)]) \right\} \quad (1)$$

where the unit of NPP_e is $\text{g C} \cdot \text{m}^{-2} \cdot \text{year}^{-1}$, t is the annual average temperature ($^{\circ}\text{C}$), and r is the annual precipitation (mm). Based on the raster calculator function of the ArcGIS v10.2 software (Environmental Systems Research Institute, Inc., Redlands, CA, USA), the monthly spatial temperature and precipitation data obtained in Section 2.2 were converted into annual data, with a spatial resolution of 250 m. Then, the annual NPP_e was estimated based on the annual spatial meteorological data, and the spatial resolution of the results were set to 250 m.

2.3.2. Estimation of the Actual NPP

The NPP_a , which is affected both by climate and human activities factors, was estimated with the CASA model [4,53]. Based on the principle of light energy use, Monteith first proposed the concept of estimating NPP based on photosynthetically active radiation (APAR) and light energy use (ϵ) in 1972 [54]. Moreover, in 1993, Potter proposed the CASA model and realized the estimation of regional

and global NPP using the principle of light energy use based on remote sensing data [55,56]. As it is possible to reflect the influence of climate and human factors on NPP, this is used widely in remote sensing retrieval research on NPP [17,32]. The main formula of the model is as follows:

$$NPP_a(x, t) = APAR(x, t) \times \varepsilon(x, t) \quad (2)$$

where $APAR(x, t)$ is the photosynthetically active radiation ($\text{g C} \cdot \text{m}^{-2} \cdot \text{month}^{-1}$) absorbed by vegetation in pixel x at time t , and $\varepsilon(x, t)$ is the actual light energy use ($\text{gC} \cdot \text{MJ}^{-1}$) of vegetation in pixel x at time t . $APAR(x, t)$ can be calculated as follows:

$$APAR(x, t) = SOL(x, t) \times 0.5 \times FPAR(x, t) \quad (3)$$

where $SOL(x, t)$ indicates the total solar radiation ($\text{MJ} \cdot \text{m}^{-2}$) in pixel x at time t , $FPAR(x, t)$ indicates the proportion of photosynthetically active radiation vegetation absorbs, and a constant of 0.5 indicates the proportion of total solar radiation (0.4–0.7 μm) available for vegetation.

The SOL were obtained from the China Meteorological Data Sharing Network (<http://data.cma.cn/>). The monthly SOL data of meteorological stations were used to calculate the spatial distribution of the SOL by using ArcGIS v10.2 software (Environmental Systems Research Institute, Inc., Redlands, CA, USA) with Kriging interpolation method. The spatial resolution of the results was set to 250 m.

FPAR can be expressed as follows:

$$FPAR = \frac{(NDVI(x, t) - NDVI_{i,\min})(FPAR_{\max} - FPAR_{\min})}{NDVI_{i,\max} - NDVI_{i,\min}} + FPAR_{\min} \quad (4)$$

where $NDVI(x, t)$ indicates the NDVI value in pixel x at time t , $NDVI_{i,\max}$ and $NDVI_{i,\min}$ are the maximum and minimum NDVI value of the vegetation type i . $FPAR_{\max}$ and $FPAR_{\min}$ are constants of 0.95 and 0.001, respectively.

$\varepsilon(x, t)$ can be calculated as follows:

$$\varepsilon(x, t) = T_{\varepsilon 1}(x, t) \times T_{\varepsilon 2}(x, t) \times W_{\varepsilon}(x, t) \times \varepsilon_{\max} \quad (5)$$

where $T_{\varepsilon 1}(x, t)$ and $T_{\varepsilon 2}(x, t)$ are the temperature stress coefficients at low and high temperatures, $W_{\varepsilon}(x, t)$ is the water stress coefficient, and ε_{\max} is the maximum light energy conversion rate under ideal conditions, which is $0.389 \text{ g C} \cdot \text{MJ}^{-1}$.

$T_{\varepsilon 1}(x, t)$ and $T_{\varepsilon 2}(x, t)$ can be presented as follows:

$$T_{\varepsilon 1}(x, t) = 0.8 + 0.02 \cdot T_{opt}(x) - 0.0005 \cdot [T_{opt}(x)]^2 \quad (6)$$

$$T_{\varepsilon 2}(x, t) = 1.184 / \{1 + \exp[0.2 \cdot (T_{opt}(x) - 10 - T(x, t))]\} \cdot 1 / \{1 + \exp[0.3 \cdot (-T_{opt}(x) - 10 + T(x, t))]\} \quad (7)$$

where $T_{opt}(x)$ is the optimum temperature for vegetation growth, which is the average monthly temperature ($^{\circ}\text{C}$) when the NDVI value in pixel x reaches the maximum within one year. T is the annual average temperature ($^{\circ}\text{C}$).

$W_{\varepsilon}(x, t)$ can be calculated as follows:

$$W_{\varepsilon}(x, t) = 0.5 + 0.5 \cdot EET(x, t) / EPT(x, t) \quad (8)$$

where EET is the actual evapotranspiration (mm), EPT is the potential evapotranspiration (mm), which are both obtained from the meteorological data in Section 2.2.

The time and spatial resolution of all the parameters of the CASA model for estimating NPP are set to monthly and 250 m, respectively. The monthly NPP was calculated and then summed to the annual NPP used in this study.

2.3.3. Estimation of the NPP_h and Condition Analysis

The difference between the NPP_a and the NPP_e is the human-induced NPP (NPP_h), which is affected only by human activities. The formula can be expressed as follows:

$$NPP_h = NPP_a - NPP_e \quad (9)$$

To measure the change trend in the NPP, the ordinary least-squares regression formula was used, which is as follows:

$$Slope = \frac{\sum_{i=1}^n x_i y_i - \frac{1}{n} (\sum_{i=1}^n x_i) (\sum_{i=1}^n y_i)}{\sum_{i=1}^n x_i^2 - \frac{1}{n} (\sum_{i=1}^n x_i)^2} \quad (10)$$

where x_i is 1 to n for years 2000 to 2014, and y_i is the NPP in year x_i . Areas with a positive slope indicate that both the NPP and vegetation dynamics in these areas showed an increasing trend, while conversely, areas with a negative value indicate a decreasing trend [48,57].

Consequently, five types of possible conditions that lead to vegetation dynamics change can be defined by the slopes of the NPP_a (S_a), NPP_e (S_e), and the NPP_h (S_h) (Table 2). Combined with the effects of climate change and human activities on vegetation dynamics, Condition 1 is the vegetation with no change (NC), Condition 2 is the restoration of vegetation dominated by meteorological conditions (RDC), Condition 3 is the restoration of vegetation dominated by human activities (RDH), Condition 4 is the degradation of vegetation dominated by meteorological conditions (DDC), and Condition 5 is the degradation of vegetation dominated by human activities (DDH) [32,58,59].

Table 2. Conditions to assess the effects of climate change and human activities on vegetation dynamics.

Number	Method	Cause of Vegetation Dynamics Change
Condition 1	$S_a = 0$	the vegetation had no change (NC)
Condition 2	$S_a > 0$ and $S_e > S_h$	the restoration of vegetation dominated by climate factors (RDC)
Condition 3	$S_a > 0$ and $S_e < S_h$	the restoration of vegetation dominated by human factors (RDH)
Condition 4	$S_a < 0$ and $S_e > S_h$	the degradation of vegetation dominated by climate factors (DDC)
Condition 5	$S_a < 0$ and $S_e < S_h$	the degradation of vegetation dominated by human factors (DDH)

2.4. Correlation Coefficient and Significance Test

Correlation analysis can be used to indicate the relevance and change trend of research factors [15,60], therefore, this study used the Pearson's correlation coefficient formula to calculate the significance of the NPP change trend. The calculation formula is as follows:

$$r = \frac{n \sum_{i=1}^n x_i y_i - \sum_{i=1}^n x_i \cdot \sum_{i=1}^n y_i}{\sqrt{n \sum_{i=1}^n x_i^2 - (\sum_{i=1}^n x_i)^2} \cdot \sqrt{n \sum_{i=1}^n y_i^2 - (\sum_{i=1}^n y_i)^2}} \quad (11)$$

where x_i is 1 to n for years 2000 to 2014 ($n = 15$), and y_i is the NPP_a in year x_i , r is the Pearson's correlation coefficient for each pixel. When $r > 0$, the pixel experienced an increasing trend of NPP, while conversely, when $r < 0$, the pixel experienced a decreasing trend of NPP. When $0.514 < r < 1$ or $-1 < r < -0.514$, the pixel experienced a significant increasing or decreasing trend of NPP at the $p < 0.05$ confidence intervals.

2.5. Validating NPP

The measured aboveground NPP data included 45 sites (five plots per site) of different vegetation types. The details of the sampling time and methods can be found in [19,60]. NPP simulated by the CASA model was compared with the measured NPP (Figure 2). The result indicated that the simulated NPP showed a good correlation with the measured NPP ($R^2 = 0.8$, $p < 0.001$).

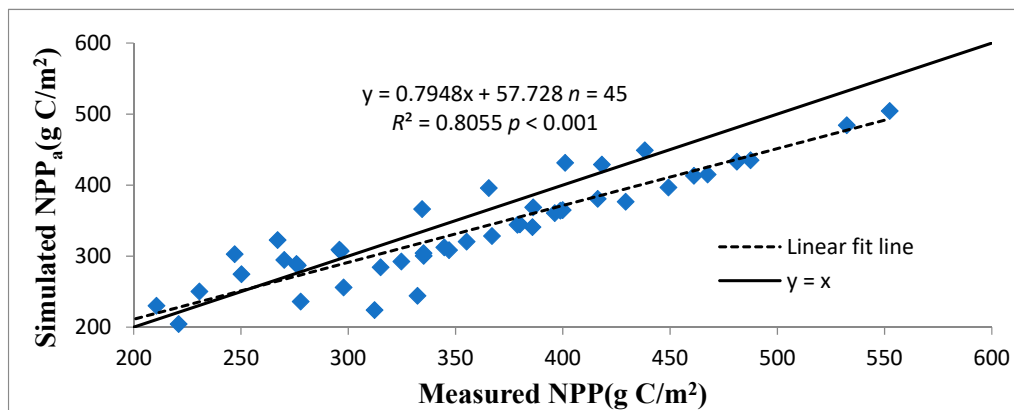


Figure 2. Comparison between the CASA model simulated NPP and the measured NPP in the Jinghe River basin. CASA model, Carnegie–Ames–Stanford Approach model; NPP, net primary productivity.

3. Results

3.1. Spatio-Temporal Trends of NPP

The annual average NPP in the Jinghe River basin from 2000 to 2014 was calculated and is shown in Figure 3. Generally, the NPP in the study area showed an increasing trend, with an increase rate of $9.438 \text{ g C} \cdot \text{m}^{-2} \cdot \text{year}^{-1}$. The highest value of annual average NPP in the 15 years was in 2014, while the lowest was in 2000. The change process can be divided into two parts: from 2000 to 2006, the NPP increased relatively moderately, then increased rapidly with fluctuations from 2007 to 2014.

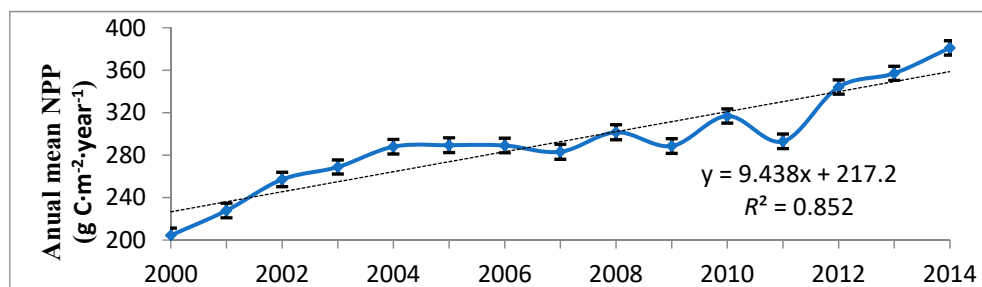


Figure 3. Interannual variations in the annual average NPP in the Jinghe River basin from 2000 to 2014.

The spatial distribution of the annual mean NPP and the change trend in the NPP are shown in Figure 4. The annual mean NPP of the Jinghe River basin showed a decreasing trend from the southeast to the northwest, which largely is consistent with the regional water and heat distribution (Figure 4a). There was a relatively clear dividing line around Weiyuan, Zhenyuan, and Heshui counties, in which the annual average NPP value was lower north of the dividing line, with the lowest value $52.6 \text{ g C} \cdot \text{m}^{-2}$, and was higher in the south, with the highest value $677.33 \text{ g C} \cdot \text{m}^{-2}$, which is more than ten times the low value and indicates obvious spatial changes.

Figure 4b shows the change trend in the NPP of the Jinghe River basin from 2000 to 2014. The results indicated that less than 0.1% of the study area showed no change trend, while 84.4% of the area showed an increasing trend. Specifically, 34.3% of the total area showed a significant increasing trend ($p < 0.05$), which was located primarily in the middle of the basin where the terrain is gentler and human activities are more frequent. Meanwhile, areas with decreasing trends in NPP accounted for 15.5% of the Jinghe River Basin area, 3.0% of which showed a significant decreasing trend ($p < 0.05$). These areas are concentrated primarily in the Ziwuling Mountain and Liupan Mountain areas on the east and west sides of the basin, respectively. The vegetations in these areas are forests and shrubs,

which had a high average value of NPP (Figure 4a). In addition, compared with the areas in which the NPP increased significantly, the terrain in these areas is relatively steep and human activities are limited.

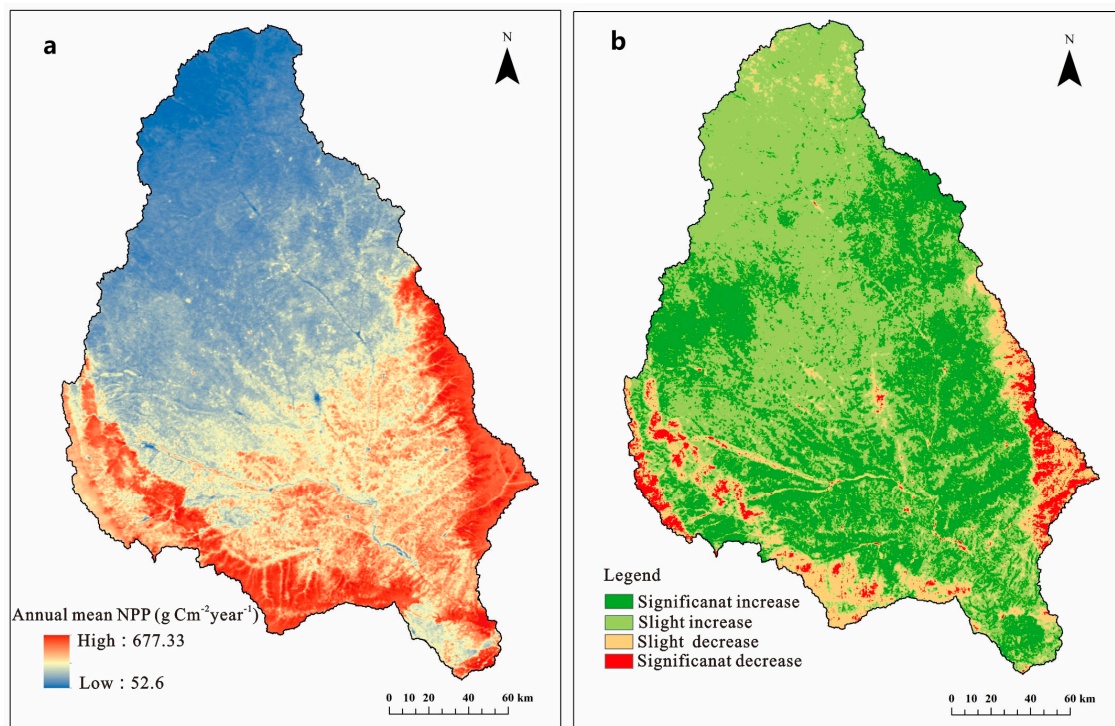


Figure 4. Spatial pattern of the mean NPP (a) and the change trend in the NPP (b) in the Jinghe River basin from 2000 to 2014.

3.2. Driving Forces in Vegetation Dynamics

The spatial pattern and area statistics of the NPP change caused by different driving factors in the Jinghe River basin from 2000 to 2014 were analyzed and are shown in Figures 5a and 6. The results indicated that human activities contributed most to the vegetation restoration in the 54.5% of the areas in which the NPP changed, which were located largely in the middle and south of the study area. Meanwhile, 24.0% of the areas in which NPP changed showed an increasing trend in the NPP that was dominated by climate factors and was located primarily in the north of the study area. Climate factors and human activities also caused vegetation degradation. Degradation dominated by human activities accounted for 4.3% of the areas in which NPP changed and were concentrated primarily in the middle of the study area. Climate factors produced 17.2% of the vegetation degradation in the areas in which NPP changed and were concentrated largely in the Ziwuling Mountain and Liupan Mountain regions.

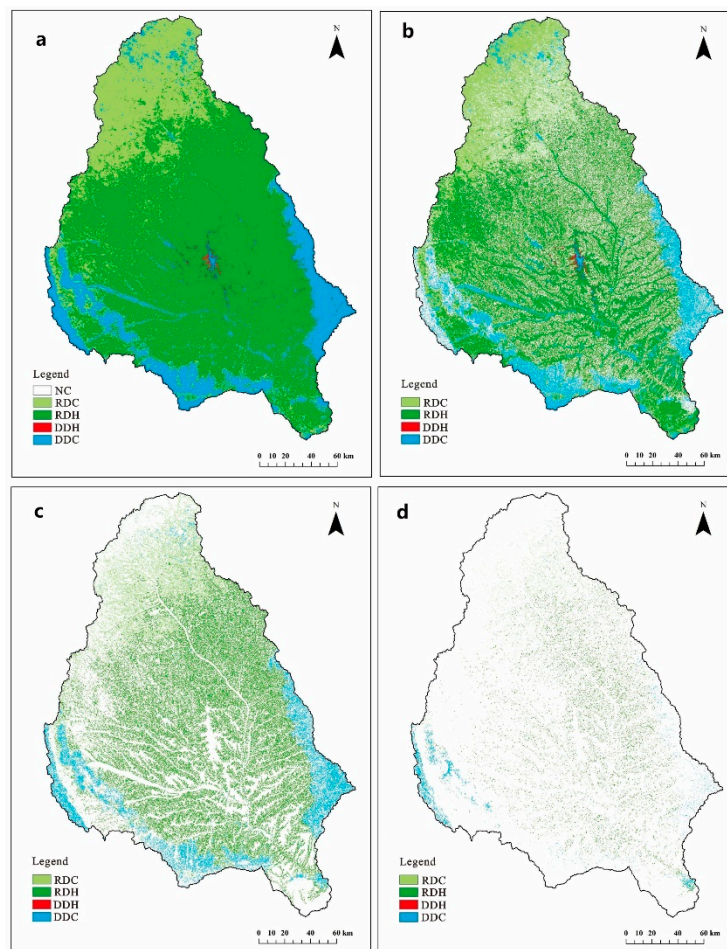


Figure 5. Spatial pattern of different conditions of the NPP change of the entire basin (a); areas with a slope less than 15° (b); areas with a slope between 15 and 25° (c); and areas with a slope greater than 25° (d) in the Jinghe River basin from 2000 to 2014. NC is the vegetation with no change, RDC is the restoration of vegetation dominated by meteorological conditions, RDH is the restoration of vegetation dominated by human activities, DDC is the degradation of vegetation dominated by meteorological conditions, DDH is the degradation of vegetation dominated by human activities.

As human activities including urban expansion and ecological restoration were closely related to topographical factors, this study adopted the requirements of the GGP to introduce topographical factors to achieve a better understanding of the spatial patterns in the NPP change trend and its driving forces. Slope gradients were divided into three levels according to the GGP requirements, slopes $<15^\circ$, those between 15 and 25° , and slopes $>25^\circ$, respectively (Figure 5b–d). The area statistics results in Figure 6 show that the positive effect of climate factors on the NPP declined continuously as the slope increased. A total of 26.6% of areas with slopes $<15^\circ$ demonstrated a restoration trend in vegetation dominated by climate factors (RDC). However, in areas with slopes $>25^\circ$, the rate decreased to only 11.9%. Furthermore, the rate of vegetation degradation in areas dominated by climate factors (DDC) increased from 16.4% to 19.6% with increasing slope. Conversely, the positive effect of human activities on the NPP continued to increase as slope increased; 52.6% of areas with slopes $<15^\circ$ indicated a restoration trend of vegetation dominated by human activities (RDH), and the rate increased to 68.4% in areas with slopes $>25^\circ$. At the same time, the rate of vegetation degradation in areas dominated by human activities (DDH) decreased from 4.4 to 0.1% with increased slope. Thus, the factors that drove vegetation dynamics changed clearly depending on the terrain.

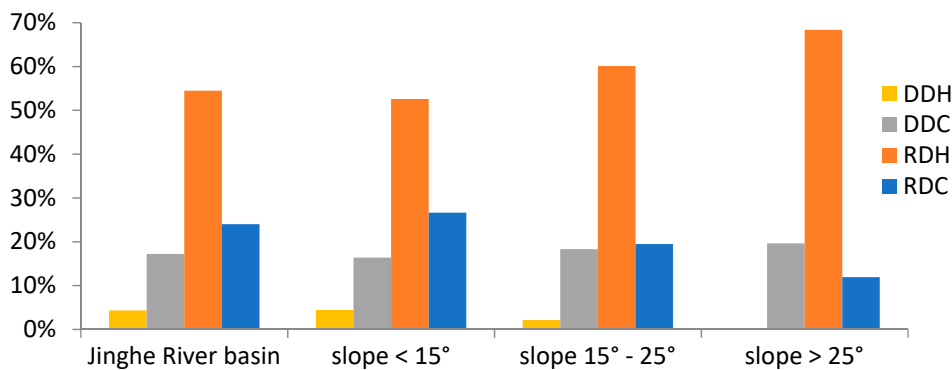


Figure 6. Area statistics of the driving factors in NPP change in the Jinghe River basin and different slopes. RDC is the restoration of vegetation dominated by meteorological conditions, RDH is the restoration of vegetation dominated by human activities, DDC is the degradation of vegetation dominated by meteorological conditions, DDH is the degradation of vegetation dominated by human activities.

4. Discussion

4.1. Methodology

Assessing the spatial patterns of the influence of climate change and human activities on vegetation dynamics accurately is of great significance in the management and restoration of regional ecological environments. However, distinguishing the effect of human activities on vegetation dynamics from those of climate factors traditionally has been difficult [40]. Several studies have adopted the NPP, which is an efficient and accurate indicator of vegetation growth status, to distinguish vegetation change dominated by human factors from that dominated by climate by comparing the difference between the expected and actual NPP [61,62]. Both the Miami and CASA models that estimate the expected and actual NPP have been used successfully in several studies at the global and regional scale [63–65]. The results of this study showed that the actual NPP in the Jinghe River basin increased from 2000 to 2014, which is consistent with previous studies and supports the feasibility of applying NPP models in this region [17,46]. Therefore, this study adopted NPP as an indicator to assess the relative roles of climate factors and human activities in vegetation change.

Although the expected and actual NPP distinguished the effects of climate factors and human activities on vegetation dynamics successfully, this method may have its own limitations. In the process of estimating the NPP expected, the Miami model includes only temperature and precipitation as the two climate factors that simulate an ideal environment of vegetation growth. Similarly, we assessed the actual NPP and the relative roles of climate and human factors in vegetation dynamics based on the NPP variation, and established conditions based on the hypothesis that vegetation dynamics is only affected by climate and human activities. However, vegetation productivity and its simulation results may be affected by several factors, such as wind, soil organic matter, vegetation types, herbivore activities, and the accuracy of the remote sensing data used in the NPP estimate models [42,66–68]. Future studies should incorporate additional driving factors based on the characteristics of the study area. Meanwhile, because of the errors inherent in the remote sensing data and the NPP simulation methods itself, there can be some errors in the NPP simulation results and the differences of NPP_e and NPP_a . However, according to previous studies, these errors may exist in the assessment of the slope, vegetation communities, and other small-scale studies. For regional and global scales, the methodology introduced in this study can be considered as a feasible method of evaluating the spatial distribution of the relative roles of climate and human activities [28,40,42].

4.2. Driving Forces

Previous studies have shown that both the NPP and vegetation in the Loess Plateau have increased significantly because of human activities, such as reducing grazing pressure and returning farmland to forests [69–71]. The results of this study confirmed that vegetation in the Jinghe River basin experienced similar change trends, with 85.5% of the vegetation in the study area showing an increasing trend. Among them, 54.5% of the increased vegetation was dominated by human activities. This rate is similar to Li's research, which indicated that human activities account for 55% of vegetation changes from 2000 to 2015 in the Loess Plateau [72]. Meanwhile, the rate of vegetation increase dominated by human activities rose with increased slope, from 52.6% in areas with slopes less than 15° to 68.4% in those with slopes greater than 25°. These areas were located primarily in valleys in the middle of the basin, where the land use changed more dramatically during the past decade [73]. These results are consistent with the implementation of a series of ecological projects, including the GGP. Under the guidance of government policies, farmland in valleys with steep slopes has been converted to grassland and forest, which enhances vegetation and soil carbon fixation effectively [72,74]. However, the study also confirmed that 4.3% of the NPP showed a decreasing trend in the Jinghe River basin that was dominated by negative human activities. These areas were concentrated largely in the middle of the study area, in which Qingyang city is located and has the largest population density in the Jinghe River basin. Because of its rapid population growth, the pace of urbanization has accelerated significantly and has led to drastic changes in the local environment around the city that have decreased the vegetation cover and carbon fixation [60,75].

Changes in climate factors are another important force that affects the vegetation dynamics, and the vegetation changes in the Jinghe River basin that climate forcing dominated showed clear spatial characteristics. The results of this study indicated that vegetation restoration dominated by climate factors in the study area is distributed primarily in the northern part of the basin (Figure 5a). Based on the zonal statistics results of the spatial annual temperature and precipitation data in the Jinghe River basin from 2000 to 2014, the annual mean temperature in the study area is between 7.8 to 12.5 °C and increased at a change rate of 0.2 °C/10 year; while the annual precipitation is between 334.2 to 620.8 mm and decreased at a change rate of 24 mm/10 year over the past 15 years, respectively (Figures 7 and 8). These results indicate that the climate in the study area is becoming warmer and drier, which leads to drought, as Li et al. and Zhao et al. reported [76,77]. In a water-limited area, the spatial distribution of precipitation determines the vegetation distribution and growth [9]. Zhang et al. pointed out that, compared with other areas that suffered drought, precipitation in the northern part of the Jinghe River basin is relatively sufficient, which is likely to be the reason that vegetation restoration dominated by climate factors is concentrated in that area [78].

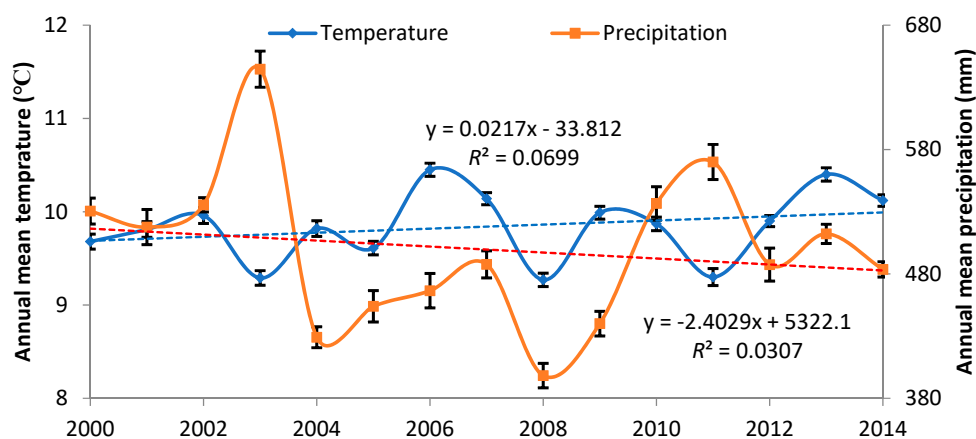


Figure 7. Interannual variations in the annual mean temperature and annual precipitation in the Jinghe River basin from 2000 to 2014.

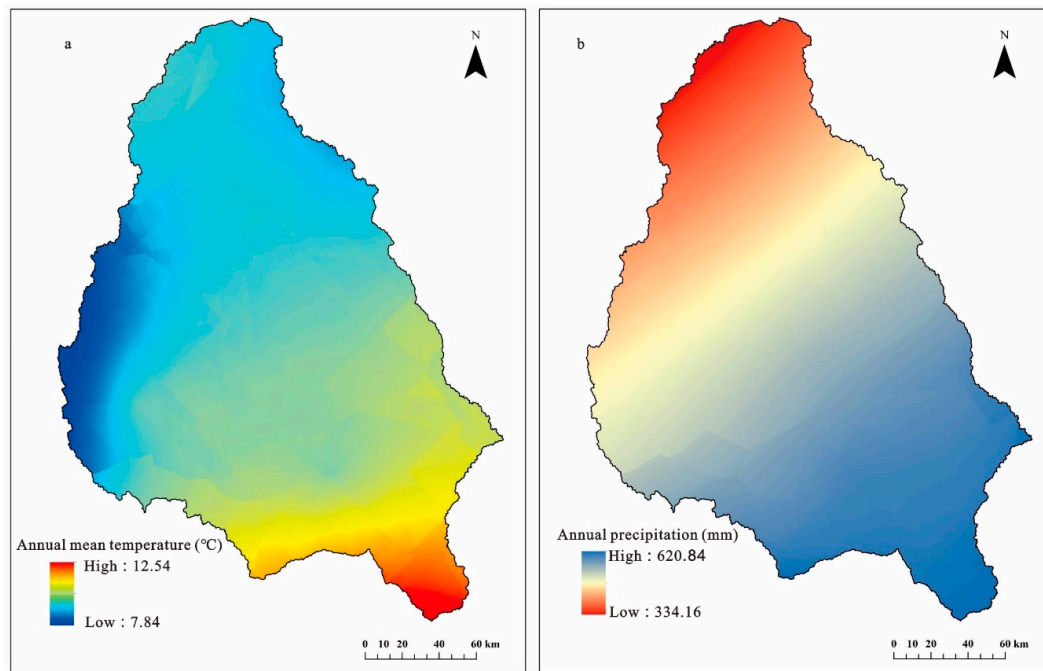


Figure 8. Spatial pattern of the annual mean temperature (a) and the annual precipitation (b) in the Jinghe River basin from 2000 to 2014.

The vegetation degradation dominated by climate factors was located generally in the Ziwuling Mountain and Liupan Mountain regions on the east and west sides of the basin, respectively. Because of the drought climate, the vegetation in the mountain areas showed significant vegetation degradation dominated by climatic factors. Although ecological restoration measures, such as returning farmland to forests and protecting vegetation, also must be implemented in these areas, the terrain there restricts follow-up human management activities such as irrigation. Therefore, the water demand of the vegetation in the mountain areas relies primarily on natural precipitation and soil moisture [19,79]. However, vegetation planted recently has increased the local water demand and accelerated the consumption of regional water resources, which eventually had led to degradation of the vegetation [80,81].

5. Conclusions

This study assessed the driving forces in vegetation dynamics in the Jinghe River basin from 2000 to 2014 using NPP as the indicator. The results showed that the vegetation increased in the study area, and human activities played an active role in the vegetation restoration, especially in valleys in the middle of the basin, where the rate of vegetation change in the areas dominated by human activities rose continuously with the increase in slope. This result is consistent with the implementation of ecological projects such as GGP. The degradation of vegetation caused by human activities was located primarily in populous areas and was related closely to urban expansion. The vegetation restoration that was dominated by climate factors was concentrated largely in the northern part of the basin, where the precipitation was relatively sufficient. However, the vegetation degradation dominated by climate factors generally was located in the Ziwuling Mountain and Liupan Mountain regions on the east and west sides of the basin, where the vegetation degradation rate in areas attributable to climate factors rose with increases in slope. In these regions, the arid climate caused a shortage of water resources, and the human dominated vegetation restoration activities exacerbated the water demand of vegetation further and surpassed the carrying capacity of the regional water resources, which led ultimately to vegetation degradation.

The methodology of comparing the expected and actual NPP to distinguish the effect of climate factors and human activities on vegetation dynamics in this study demonstrated a relatively higher accuracy and can be applied at different regional scales. Further, as unsustainable vegetation restoration measures may cause regional imbalances in water supply, and lead eventually to vegetation degradation, we recommend that future ecological restoration programs pay more attention to maintaining the balance between ecosystem restoration and water resource demands to maximize the benefits of human activities and ensure that the vegetation restoration is ecologically sustainable.

Author Contributions: H.W. analyzed the related data and wrote the manuscript; G.L. and Z.L. designed the framework of the research and revised the manuscript; and P.W. and Z.W. provided the climate and NDVI data.

Acknowledgments: This research was funded by the Science and Technology Service Network Initiative Project of Chinese Academy of Sciences (No. KFJ-STZ-ZDTP-036), the National Key R&D Program of China (2017YFC0504701), Fundamental Research Funds for the Central Universities (No. GK201703053), China Postdoctoral Science Foundation (No. 2017M623114).

Conflicts of Interest: The authors declare no conflict of interest.

References

1. Field, C.B. Global change. Sharing the garden. *Science* **2001**, *294*, 2490–2491. [[CrossRef](#)] [[PubMed](#)]
2. Root, T.L.; Price, J.T.; Hall, K.R.; Schneider, S.H.; Rosenzweig, C.; Pounds, J.A. Fingerprints of global warming on wild animals and plants. *Nature* **2003**, *421*, 47–60. [[CrossRef](#)] [[PubMed](#)]
3. Li, A.; Wu, J.G.; Huang, J.H. Distinguishing between human-induced and climate-driven vegetation changes: A critical application of RESTREND in Inner Mongolia. *Landsc. Ecol.* **2012**, *27*, 969–982. [[CrossRef](#)]
4. Zhang, Y.; Zhang, C.; Wang, Z.; Chen, Y.; Gang, C.; An, R.; Li, J. Vegetation dynamics and its driving forces from climate change and human activities in the Three-River Source Region, China from 1982 to 2012. *Sci. Total Environ.* **2016**, *563–564*, 210–220. [[CrossRef](#)] [[PubMed](#)]
5. Ma, W.; Wang, X.; Zhou, N.; Jiao, L. Relative importance of climate factors and human activities in impacting vegetation dynamics during 2000–2015 in the Otindag Sandy Land, northern China. *J. Arid Land* **2017**, *9*, 558–567. [[CrossRef](#)]
6. Huang, K.; Zhang, Y.; Zhu, J.; Liu, Y.; Zu, J.; Zhang, J. The Influences of Climate Change and Human Activities on Vegetation Dynamics in the Qinghai-Tibet Plateau. *Remote Sens.* **2016**, *8*, 876. [[CrossRef](#)]
7. Wessels, K.J.; Prince, S.D.; Malherbe, J.; Small, J.; Frost, P.E.; VanZyl, D. Can human-induced land degradation be distinguished from the effects of rainfall variability? A case study in South Africa. *J. Arid Environ.* **2007**, *68*, 271–297. [[CrossRef](#)]
8. Yao, J.Q.; Yang, Q.; Chen, Y.N. Climate change in arid areas of Northwest China in past 50 years and its effects on the local ecological environment. *Chin. J. Ecol.* **2013**, *32*, 1283–1291.
9. Wang, H.; Liu, G.H.; Li, Z.S.; Ye, X.; Wang, M.; Gong, L. Driving force and changing trends of vegetation phenology in the Loess Plateau of China from 2000 to 2010. *J. Mt. Sci.* **2016**, *13*, 844–856. [[CrossRef](#)]
10. An, R.; Wang, H.L.; Feng, X.Z.; Wu, H.; Wang, Z.; Wang, Y.; Shen, X.J.; Lu, C.H.; Quayle-Ballard, J.A.; Chen, Y.H.; et al. Monitoring rangeland degradation using a novel local NPP scaling based scheme over the “Three-River Headwaters” region, hinterland of the Qinghai-Tibetan Plateau. *Quat. Int.* **2017**, *444*, 97–114. [[CrossRef](#)]
11. Zhang, B.; Wu, P.; Zhao, X.; Wang, Y.; Gao, X. Changes in vegetation condition in areas with different gradients (1980–2010) on the Loess Plateau, China. *Environ. Earth Sci.* **2012**, *68*, 2427–2438. [[CrossRef](#)]
12. Zhang, J.; Wang, T.; Ge, J. Assessing Vegetation Cover Dynamics Induced by Policy-Driven Ecological Restoration and Implication to Soil Erosion in Southern China. *PLoS ONE* **2015**, *10*, e0131352. [[CrossRef](#)] [[PubMed](#)]
13. Yang, H.F.; Yao, L.; Wang, Y.D.; Li, J.L. Relative contribution of climate change and human activities to vegetation degradation and restoration in North Xinjiang, China. *Rangel. J.* **2017**, *39*, 289–302. [[CrossRef](#)]
14. Cao, S.; Chen, L.; Shankman, D.; Wang, C.; Wang, X.; Zhang, H. Excessive reliance on afforestation in China’s arid and semi-arid regions: Lessons in ecological restoration. *Earth-Sci. Rev.* **2011**, *104*, 240–245. [[CrossRef](#)]

15. Wang, H.; Liu, G.; Li, Z.; Ye, X.; Fu, B.; Lü, Y. Analysis of the Driving Forces in Vegetation Variation in the Grain for Green Program Region, China. *Sustainability* **2017**, *9*, 1853. [[CrossRef](#)]
16. Wang, H.; Liu, G.; Li, Z.; Ye, X.; Fu, B.; Lv, Y. Impacts of Drought and Human Activity on Vegetation Growth in the Grain for Green Program Region, China. *Chin. Geogr. Sci.* **2018**, *28*, 470–481. [[CrossRef](#)]
17. Feng, X.; Fu, B.; Lu, N.; Zeng, Y.; Wu, B. How ecological restoration alters ecosystem services: An analysis of carbon sequestration in China's Loess Plateau. *Sci. Rep.* **2013**, *3*, 2846. [[CrossRef](#)] [[PubMed](#)]
18. Deng, L.; Shangguan, Z.P.; Sweeney, S. "Grain for Green" driven land use change and carbon sequestration on the Loess Plateau, China. *Sci. Rep.* **2014**, *4*, 7039. [[CrossRef](#)] [[PubMed](#)]
19. Feng, X.M.; Fu, B.J.; Piao, S.L.; Wang, S.; Ciais, P.; Zeng, Z.Z.; Lv, Y.H.; Zeng, Y.; Li, Y.; Jiang, X.H.; et al. Revegetation in China's Loess Plateau is approaching sustainable water resource limits. *Nat. Clim. Chang.* **2016**, *6*, 1019–1022. [[CrossRef](#)]
20. Wang, Y.; Cao, S. Carbon sequestration may have negative impacts on ecosystem health. *Environ. Sci. Technol.* **2011**, *45*, 1759–1760. [[CrossRef](#)] [[PubMed](#)]
21. Cao, S.; Chen, L.; Yu, X. Impact of China's Grain for Green Project on the landscape of vulnerable arid and semi-arid agricultural regions: A case study in northern Shaanxi Province. *J. Appl. Ecol.* **2009**, *46*, 536–543. [[CrossRef](#)]
22. Wang, X.M.; Zhang, C.X.; Hasi, E.; Dong, Z.B. Has the Three Norths Forest Shelterbelt Program solved the desertification and dust storm problems in arid and semiarid China? *J. Arid Environ.* **2010**, *74*, 13–22. [[CrossRef](#)]
23. Aldous, A.; Fitzsimons, J.; Richter, B.; Bach, L. Droughts, floods and freshwater ecosystems: Evaluating climate change impacts and developing adaptation strategies. *Mar. Freshw. Res.* **2011**, *62*, 223–231. [[CrossRef](#)]
24. Lawler, J.J. Climate change adaptation strategies for resource management and conservation planning. *Ann. N. Y. Acad. Sci.* **2009**, *1162*, 79–98. [[CrossRef](#)] [[PubMed](#)]
25. Chang, X.L.; Lu, C.X.; Gao, Y.B. Impacts of human economic activities on wind and sand environment in Kerqin sandy land. *Resour. Sci.* **2003**, *25*, 78–83. (In Chinese)
26. Ma, Y.H.; Fan, S.Y.; Zhou, L.H.; Dong, Z.H.; Zhang, K.C.; Feng, J.M. The temporal change of driving factors during the course of land desertification in arid region of North China: The case of Minqin County. *Environ. Geol.* **2007**, *51*, 999–1008. [[CrossRef](#)]
27. Zhang, Y.S.; Wang, L.X.; Zhang, H.Q.; Li, X.Y. Influence of environmental factor changes on desertification process in Shule River. *Resour. Sci.* **2003**, *25*, 60–65. (In Chinese)
28. Gang, C.; Zhou, W.; Chen, Y.; Wang, Z.; Sun, Z.; Li, J.; Qi, J.; Odeh, I. Quantitative assessment of the contributions of climate change and human activities on global grassland degradation. *Environ. Earth Sci.* **2014**, *72*, 4273–4282. [[CrossRef](#)]
29. Evans, J.; Geerken, R. Discrimination between climate and human-induced dryland degradation. *J. Arid Environ.* **2004**, *57*, 535–554. [[CrossRef](#)]
30. Prince, S.D.; Wessels, K.J.; Tucker, C.J.; Nicholson, S.E. Desertification in the Sahel: A reinterpretation of a reinterpretation. *Glob. Chang. Biol.* **2007**, *13*, 1308–1313. [[CrossRef](#)]
31. Wessels, K.J.; Prince, S.D.; Frost, P.E.; Zyl, D. Assessing the effects of human-induced land degradation in the former homelands of northern South Africa with a 1 km AVHRR NDVI time-series. *Remote Sens. Environ.* **2004**, *91*, 47–67. [[CrossRef](#)]
32. Chen, B.; Zhang, X.; Tao, J.; Wu, J.; Wang, J.; Shi, P.; Zhang, Y.; Yu, C. The impact of climate change and anthropogenic activities on alpine grassland over the Qinghai-Tibet Plateau. *Agric. For. Meteorol.* **2014**, *189–190*, 11–18. [[CrossRef](#)]
33. Wessels, K.J.; Prince, S.D.; Reshef, I. Mapping land degradation by comparison of vegetation production to spatially derived estimates of potential production. *J. Arid Environ.* **2008**, *72*, 1940–1949. [[CrossRef](#)]
34. Yeganeh, H.; Khajedain, S.J.; Amiri, F.; Shariff, A.R.B.M. Monitoring rangeland ground cover vegetation using multitemporal MODIS data. *Arabian J. Geosci.* **2014**, *7*, 287–298. [[CrossRef](#)]
35. Zheng, Y.R.; Xie, Z.X.; Robert, C.; Jiang, L.H.; Shimizu, H. Did climate drive ecosystem change and induce desertification in Otindag sandy land, China over the past 40 years? *J. Arid Environ.* **2006**, *64*, 523–541. [[CrossRef](#)]

36. Wang, H.; Liu, G.; Li, Z.; Ye, X.; Wang, M.; Gong, L. Impacts of climate change on net primary productivity in arid and semiarid regions of China. *Chin. Geogr. Sci.* **2015**, *26*, 35–47. [[CrossRef](#)]
37. Nemani, R.R.; Keeling, C.D.; Hashimoto, H.; Jolly, W.M.; Piper, S.C.; Tucker, C.J.; Myneni, R.B.; Running, S.W. Climate driven increases in global terrestrial net primary production from 1982 to 1999. *Science* **2003**, *300*, 1560–1563. [[CrossRef](#)] [[PubMed](#)]
38. Li, S.; Yan, J.; Liu, X.; Wan, J. Response of vegetation restoration to climate change and human activities in Shaanxi-Gansu-Ningxia Region. *J. Geogr. Sci.* **2013**, *23*, 98–112. [[CrossRef](#)]
39. Haberl, H.; Krausmann, F.; Erb, K.; Schulz, N.B. Human Appropriation of Net Primary Production. *Science* **2002**, *296*, 1968–1969. [[CrossRef](#)] [[PubMed](#)]
40. Zhou, W.; Gang, C.; Zhou, F.; Li, J.; Dong, X.; Zhao, C. Quantitative assessment of the individual contribution of climate and human factors to desertification in northwest China using net primary productivity as an indicator. *Ecol. Indic.* **2015**, *48*, 560–569. [[CrossRef](#)]
41. Haberl, H.; Erb, K.; Krausmann, F.; Gaube, V.; Bondeau, A.; Plutzer, C.; Gingrich, S.; Lucht, W.; Fischer-Kowalski, M. Quantifying and Mapping the Human Appropriation of Net Primary Production in Earth's Terrestrial Ecosystems. *Proc. Natl. Acad. Sci. USA* **2007**, *104*, 12942–12947. [[CrossRef](#)] [[PubMed](#)]
42. Yang, Y.; Wang, Z.; Li, J.; Gang, C.; Zhang, Y.; Zhang, Y.; Odeh, I.; Qi, J. Comparative assessment of grassland degradation dynamics in response to climate variation and human activities in China, Mongolia, Pakistan and Uzbekistan from 2000 to 2013. *J. Arid Environ.* **2016**, *135*, 164–172. [[CrossRef](#)]
43. Xu, D.; Kang, X.; Liu, Z.; Zhuang, D.; Pan, J. Assessing the relative role of climate change and human activities in sandy desertification of Ordos region, China. *Sci. China* **2009**, *52*, 855–868. (In Chinese) [[CrossRef](#)]
44. Xie, F.; Qiu, G.; Yin, J.; Xiong, Y.J.; Wang, P. Comparison of Land Use/Land Cover Change in Three Sections of the Jinghe River Basin between the 1970s and 2006. *J. Nat. Resour.* **2009**, *24*, 1354–1365. (In Chinese)
45. Yue, D.X.; Du, J.; Liu, J.Y.; Gou, J.J.; Zhang, J.J.; Ma, J.H. Spatio-temporal analysis of ecological carrying capacity in Jinghe Watershed based on Remote Sensing and Transfer Matrix. *Acta Ecol. Sin.* **2011**, *31*, 2550–2558. (In Chinese)
46. Qi, Q.; Wang, T.; Kou, X.J.; Ge, J.P. Temporal and spatial changes of vegetation cover and the relationship with precipitation in Jinghe watershed of china. *J. Plant Ecol.* **2009**, *33*, 246–253. (In Chinese)
47. Zhang, Y.S.; Chen, X.; Gao, M.; Zhang, Z.C.; Cheng, Q.B. Detecting Temporal Variations of Temperature Characteristics in Jinghe Watershed. *J. Water Resour. Res.* **2017**, *6*, 33–41. (In Chinese) [[CrossRef](#)]
48. Slayback, D.A.; Pinzon, J.E.; Los, S.O.; Tucker, C.J. Northern hemisphere photosynthetic trends 1982–99. *Glob. Chang. Biol.* **2003**, *9*, 1–15. [[CrossRef](#)]
49. Wang, X.; Piao, S.L.; Ciais, P.; Li, J.; Friedlingstein, P.; Koven, C.; Chen, A. Spring temperature change and its implication in the change of vegetation growth in North America from 1982 to 2006. *Proc. Natl. Acad. Sci. USA* **2011**, *108*, 1240–1245. [[CrossRef](#)] [[PubMed](#)]
50. Lieth, H. Primary production: Terrestrial ecosystems. *Hum. Ecol.* **1973**, *1*, 303–332. [[CrossRef](#)]
51. Lin, H.; Feng, Q.; Liang, T.; Ren, J. Modelling global-scale potential grassland changes in spatio-temporal patterns to global climate change. *Int. J. Sustain. Dev. World Ecol.* **2012**, *20*, 83–96. [[CrossRef](#)]
52. Adams, B.; White, A.; Lenton, T.M. An analysis of some diverse approaches to modelling terrestrial net primary productivity. *Ecol. Model.* **2004**, *177*, 353–391. [[CrossRef](#)]
53. Mu, S.; Zhou, S.; Chen, Y.; Li, J.; Ju, W.; Odeh, I.O.A. Assessing the impact of restoration-induced land conversion and management alternatives on net primary productivity in Inner Mongolian grassland, China. *Glob. Planet. Chang.* **2013**, *108*, 29–41. [[CrossRef](#)]
54. Monteith, J.L. Solar Radiation and Productivity in Tropical Exosystems. *J. Appl. Ecol.* **1972**, *9*, 747–766. [[CrossRef](#)]
55. Potter, C.S.; Randerson, J.T.; Field, C.B.; Matson, P.A.; Vitousek, P.M.; Mooney, H.A.; Klooster, S.A. Terrestrial ecosystem production: A process model based on global satellite and surface data. *Glob. Biogeochem. Cycles* **1993**, *7*, 811–841. [[CrossRef](#)]
56. Wen, Y.; Liu, X.; Du, G. Nonuniform Time-Lag Effects of Asymmetric Warming on Net Primary Productivity across Global Terrestrial Biomes. *Earth Interact.* **2018**, *22*, 1–26. [[CrossRef](#)]
57. Shi, Y.; Shen, Y.; Kang, E.; Li, D.; Ding, Y.; Zhang, G.; Hu, R. Recent and Future Climate Change in Northwest China. *Clim. Chang.* **2006**, *80*, 379–393. [[CrossRef](#)]

58. Zhang, C.X.; Wang, X.; Li, J.C.; Hua, T. Roles of climate changes and human interventions in land degradation: A case study by net primary productivity analysis in China's Shiyanghe Basin. *Environ. Earth Sci.* **2011**, *64*, 2183–2193. [[CrossRef](#)]
59. Zhou, W.; Li, J.; Mu, S.J.; Gang, C.C.; Sun, Z.G. Effects of ecological restoration-induced land-use change and improved management on grassland net primary productivity in the Shiyanghe River Basin, north-west China. *Grass Forage Sci.* **2013**, *10*, 1111. [[CrossRef](#)]
60. Lu, Y.; Fu, B.; Feng, X.; Zeng, Y.; Liu, Y.; Chang, R.; Sun, G.; Wu, B. A policy-driven large scale ecological restoration: Quantifying ecosystem services changes in the Loess Plateau of China. *PLoS ONE* **2012**, *7*, e31782.
61. Wu, S.H.; Zhou, S.L.; Chen, D.X.; Wei, Z.Q.; Dai, L.; Li, X.G. Determining the contributions of urbanisation and climate change to NPP variations over the last decade in the Yangtze River Delta, China. *Sci. Total Environ.* **2014**, *472*, 397–406. [[CrossRef](#)] [[PubMed](#)]
62. Mu, S.J.; Chen, Y.Z.; Li, J.L.; Ju, W.M.; Odeh, I.O.A.; Zou, X.L. Grassland dynamics in response to climate change and human activities in Inner Mongolia, China between 1985 and 2009. *Rangel. J.* **2013**, *35*, 315–329. [[CrossRef](#)]
63. Zhu, W.Q.; Pan, Y.Z.; Zhang, J.S. Estimation of net primary productivity of Chinese terrestrial vegetation based on remote sensing. *J. Plant Ecol.* **2007**, *31*, 413–424. (In Chinese)
64. Yu, D.Y.; Shi, P.J.; Shao, H.B.; Zhu, W.Q.; Pan, Y.Z. Modelling net primary productivity of terrestrial ecosystems in East Asia based on an improved CASA ecosystem model. *Int. J. Remote Sens.* **2009**, *30*, 4851–4866. [[CrossRef](#)]
65. Zaks, D.P.; Ramankutty, N.; Barford, C.C.; Foley, J.A. From Miami to Madison: Investigating the relationship between climate and terrestrial net primary production. *Glob. Biogeochem. Cycles* **2007**, *21*, GB3004. [[CrossRef](#)]
66. Cao, X.; Gu, Z.H.; Chen, J.; Liu, J.; Shi, P.J. Analysis of human-induced steppe degradation based on remote sensing in Xilin Gole, Inner Mongolia, China. *J. Plant Ecol.* **2006**, *30*, 268–277. (In Chinese)
67. Yi, L.; Ren, Z.Y.; Zhang, C.; Liu, W. Vegetation cover, climate and human activities on the loess plateau. *Resour. Sci.* **2014**, *36*, 166–174. (In Chinese)
68. Wang, Q.; Zhang, B.; Dai, S.P.; Zhang, F.F.; Zhao, Y.F.; Yin, H.X.; He, X.Q. Analysis of the vegetation cover change and its relationship with factors in the Three-North Shelter Forest Program. *China Environ. Sci.* **2012**, *32*, 1302–1308. (In Chinese)
69. Su, C.; Fu, B. Evolution of ecosystem services in the Chinese Loess Plateau under climatic and land use changes. *Glob. Planet. Chang.* **2013**, *101*, 119–128. [[CrossRef](#)]
70. Wang, Y.; Fu, B.; Lü, Y.; Chen, L. Effects of vegetation restoration on soil organic carbon sequestration at multiple scales in semi-arid Loess Plateau, China. *Catena* **2011**, *85*, 58–66. [[CrossRef](#)]
71. Li, S.; Liang, W.; Fu, B.; Lu, Y.; Fu, S.; Wang, S.; Su, H. Vegetation changes in recent large-scale ecological restoration projects and subsequent impact on water resources in China's Loess Plateau. *Sci. Total Environ.* **2016**, *569–570*, 1032–1039. [[CrossRef](#)] [[PubMed](#)]
72. Li, J.; Peng, S.; Li, Z. Detecting and attributing vegetation changes on China's Loess Plateau. *Agric. For. Meteorol.* **2017**, *247*, 260–270. [[CrossRef](#)]
73. Li, J.; Li, Z.; Lü, Z. Analysis of spatiotemporal variations in land use on the Loess Plateau of China during 1986–2010. *Environ. Earth Sci.* **2016**, *75*, 997. [[CrossRef](#)]
74. Deng, L.; Liu, G.B.; Shanguan, Z.P. Land-use conversion and changing soil carbon stocks in China's 'Grain-for-Green' Program: A synthesis. *Glob. Chang. Biol.* **2014**, *20*, 3544–3556. [[CrossRef](#)] [[PubMed](#)]
75. Luck, G.W.; Smallbone, L.T.; O'Brien, R. Socio-Economics and Vegetation Change in Urban Ecosystems: Patterns in Space and Time. *Ecosystems* **2009**, *12*, 604–620. [[CrossRef](#)]
76. Li, Z.; Wang, J.; Liu, W.Z. Climate Changes in Jinghe Watershed and Its Relationship with ENSO. *Prog. Geogr.* **2010**, *29*, 833–839. (In Chinese)
77. Zhao, C.; Li, Z.; Liu, W.Z. Downscaling GCMs to Project the Potential Changes of Precipitation in Jinghe Basin. *Res. Soil Water Conserv.* **2014**, *21*, 23–28. (In Chinese)
78. Zhang, H.B.; Gu, L.; Xin, C.; Yu, Q.J. Investigation on the Spatial-temporal Variation of Drought Characteristics in Jinghe River Basin. *J. North China Univ. Water Resour. Electr. Power* **2016**, *37*, 1–10. (In Chinese)
79. Lal, R. Carbon Sequestration in Dryland Ecosystems. *Environ. Manag.* **2004**, *33*, 528–544. [[CrossRef](#)] [[PubMed](#)]

80. Wang, H.S.; Huang, M.; Zhang, L. Impacts of re-vegetation on water cycle in a small watershed of the Loess Plateau. *J. Nat. Resour.* **2004**, *19*, 344–350.
81. Tian, F.; Feng, X.; Zhang, L.; Fu, B.; Wang, S.; Lv, Y.; Wang, P. Effects of revegetation on soil moisture under different precipitation gradients in the Loess Plateau, China. *Hydrol. Res.* **2017**, *48*, 1378–1390. [[CrossRef](#)]



© 2018 by the authors. Licensee MDPI, Basel, Switzerland. This article is an open access article distributed under the terms and conditions of the Creative Commons Attribution (CC BY) license (<http://creativecommons.org/licenses/by/4.0/>).